universe

IMPACT FACTOR 2.5

CITESCORE 4.3

Communication

Identifying a Point-Symmetrical Morphology in the Core-Collapse Supernova Remnant W44

Noam Soker

MDPI

https://doi.org/10.3390/universe11010004

universe

MDPI

Communication

Identifying a Point-Symmetrical Morphology in the Core-Collapse Supernova Remnant W44

Noam Soker

Department of Physics, Technion-Israel Institute of Technology, Haifa 3200003, Israel; soker@physics.technion.ac.il

Abstract: I identify a point-symmetrical morphology in the core-collapse supernova remnant (CCSNR) W44 compatible with shaping by three or more pairs of jets in the jittering jets explosion mechanism (JJEM). Motivated by recent identifications of point-symmetrical morphologies in CCSNRs and their match to the JJEM, I revisit the morphological classification of CCSNR W44. I examine a radio map of W44 and find the outer bright rim of the radio map to possess a point-symmetric structure compatible with shaping by two energetic pairs of opposite jets rather than an S-shaped morphology shaped by a precessing pair of jets. An inner pair of filaments might hint at a third powerful pair of jets. More pairs of jets were involved in the explosion process. This study adds to the growing evidence that the JJEM is the primary explosion mechanism of core-collapse supernovae.

Keywords: supernovae: general; stars: jets; ISM: supernova remnants; stars: massive

1. Introduction

The jittering jets explosion mechanism (JJEM) is a theoretical mechanism for exploding core-collapse supernovae (CCSNe), in which several to a few tens of pairs of jets explode the star. Intermittent accretion disks around the newly born neutron star (NS) launch the exploding jets in stochastically varying directions and powers (e.g., [1–5]; for recent quantitative values of the different parameters of the JJEM, see [6]). Most jets are choked inside the core, deposit their energy, and explode the star. Some pairs of jets might leave imprints on the CCSN remnant (CCSNR), e.g., by forming dense clumps, inflating bubbles or ears, breaking out through the main ejecta, and leaving behind a nozzle.

Since the intermittent accretion disks launch pairs of opposite jets, these structural features come in pairs. Pairs of structural features not along the same line form a point-symmetric morphology. As such, the JJEM predicts that many CCSNRs possess point-symmetric morphologies, but not all CCSNRs. The recent identification of point-symmetric morphologies in more than ten CCSNRs confirms one of the fundamental predictions of the JJEM (for a review of 2024 results and list of the point-symmetric CCSNe, see [7]).

The effect of the NS natal kick, instabilities during the explosion process, and the interaction of the ejecta with a circumstellar material and the interstellar medium cannot account for all properties of the identified point-symmetric morphologies of these CCSNRs [8]. These processes smear any point-symmetrical morphology. These make it challenging to identify point-symmetrical morphologies in some cases. For these challenging identifications, any additional CCSNR with an identified point-symmetric morphology is a treasure to JJEM researchers.

The magnetorotational explosion mechanism (e.g., [9–14]), which is an active topic of research (e.g., [15–17]), requires the pre-collapse core to have a fast rotation; after the explosion, it has one fixed axis of symmetry. Because it has one fixed axis of symmetry, the

check for updates

Academic Editor: Denis Leahy

Received: 11 November 2024
Revised: 20 December 2024
Accepted: 24 December 2024
Published: 26 December 2024

Citation: Soker, N. Identifying a Point-Symmetrical Morphology in the Core-Collapse Supernova Remnant W44. *Universe* **2025**, *11*, 4. https://doi.org/10.3390/universe11010004

magnetorotational explosion mechanism cannot explain point-symmetric CCSNRs with two or more symmetry axes. Also, because it requires rapid pre-collapse core rotation (e.g., [18]), this mechanism operates only in rare cases, i.e., ≃1% of CCSNe, (e.g., [19]); this mechanism assumes that most CCSNe are jetless and explode by the neutrino-driven explosion mechanism.

Spin-kick alignment is observed in many pulsars (e.g., [20–22]). Both the magnetorotational explosion mechanism (e.g., [15]) and the JJEM [23] can explain this alignment. However, while there are many simulations of the magnetorotational explosion mechanism (e.g., [15,24]), only two studies have simulated the interaction of jittering jets with the core during the explosion mechanism [1], and they are limited in their extent. Namely, the JJEM assumes the launching of jets, but there are no simulations showing the launching of jets.

As I show in this study, the CCSNR W44 (G34.7-0.4, 3C 392) is also challenging. The earlier W44 morphological classification was of an elongated structure with an S-shape morphology (Section 2). Motivated by the recent identification of point-symmetrical CCSNRs, I revisit its morphological classification and find it to be point-symmetric (Section 3). In Section 4, I discuss alternatives that cannot account for the point-symmetric morphology, and in Section 5, I summarize this short study and its significant contribution in establishing the JJEM as the primary explosion mechanism of CCSNe.

2. Previous S-Shape Classification

In this section, I discuss the previous morphological classification of W44 concerning a jet-driven explosion.

SNR W44 was mapped in several wavebands, e.g., gamma ray (e.g., [25]), X-ray (e.g., [26–30]), visible (e.g., [31–33]), IR (e.g., [34,35]), and radio (e.g., [36–41]). SNR W44 is close to the Galactic plane and interacts with a molecular cloud (e.g., [31,42–46]). It has a pulsar, PSR B1853+01 and its distance is ≃3 kpc (e.g., [47]). In Figure 1, I present a composite image of W44 from the NASA site. The image shows the complicated structure of W44, particularly its filamentary texture and unequal west–east sides. I mark the two axes of the two energetic jets that I propose shaped W44 during the explosion process (Section 3).

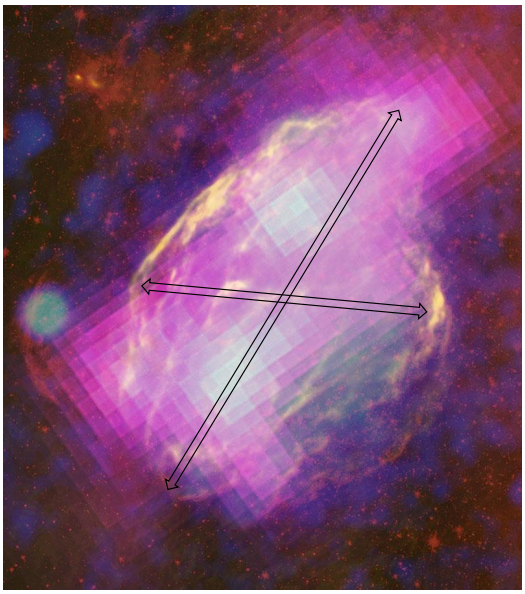

Figure 1. A composite image of CCSNR W44 from NASA site. I add two double-headed arrows that depict the two axes of the two energetic jets that I propose to have shaped W44 during the explosion process (Section 3). Magenta: GeV gamma ray from Fermi's LAT; yellow: radio from the Karl G. Jansky Very Large Array; red: infrared; blue: X-ray from ROSAT. Credit: NASA/DOE/Fermi LAT Collaboration, NRAO/AUI, JPL-Caltech, ROSAT; https://www.nasa.gov/universe/nasas-fermi-proves-supernova-remnants-produce-cosmic-rays/ (accessed on 10 November 2024).

W44 has an elongated morphology (e.g., [38]). Ref. [48] identified two ears in IR images of W44. Figure 2 is from their paper. They mark the base of each ear that they identified (thin double-headed yellow arrows), the middle of each ear (thin double-headed red arrows), and the center of W44 in the symmetrical morphology they identified (thick orange double-headed arrow). They aimed to calculate the energy of the jets that inflated the ears.

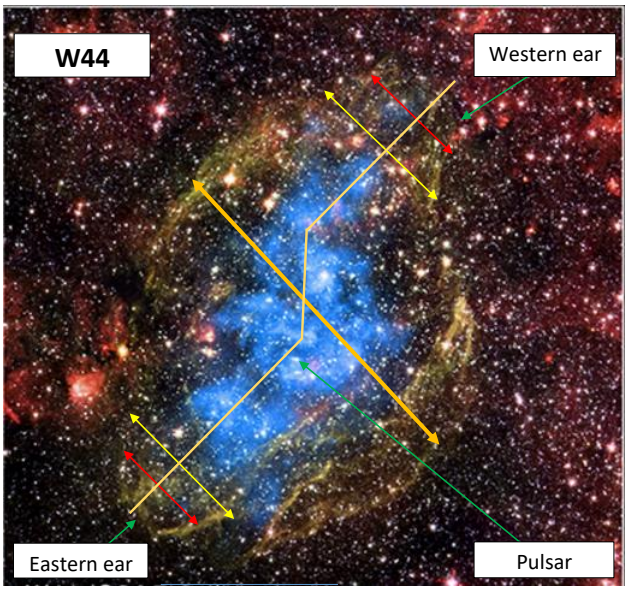

Figure 2. An image of CCSNR W44 from the Chandra gallery, with marks from [48]. Red, blue, and green colors represent infrared emission (based on NASA/JPL-Caltech; see image in [35]), and cyan represents X-ray emission (based on [27]). The red and yellow double-headed arrows mark the two opposite ears that [48] identified, and the three-segment line is the S-shape that they attributed to SNR W44.

Ref. [48] identified an S-shaped morphology, as the three-segment line on Figure 2 depicts. They also noted that the ears they defined with the S-shaped morphology appear in the IR image but not in the X-ray or radio. Motivated by identifying eleven point-symmetric CCSNRs in the past two years, I revisit the morphological classification of W44.

3. Identifying a Point-Symmetric Morphology in W44

Considering W44's complicated structure, I prefer to examine the radio map, which is the most detailed. I determine whether W44, or part of it, possesses a point-symmetric morphology.

I found the radio image from [49] to fulfill my goals; I present this image in Figure 3 (the same image in the four panels). They mark the location of six regions with strong OH (1720 MHz) emission on that image, which I do not refer to in this study. On Figure 3a, I have added two red arrows pointing at the structural features I term dents, where the bright rim sharply bends inward.

In Figure 3b, I mark several western structural features. I draw a line (orange) on the bright western rim of W44. I mark three structural features outside and attached to the rim on the west (dashed pale blue lines). I draw a dotted yellow line on an inner filament on the southwest. The yellow double-headed arrow points at the two dents. One double-line double-headed red arrow is along the long dimension of W44, through the center of the point-symmetrical structure that I mark with an asterisk; the other goes through the center and points at two opposite protrusions of the bright rim. The centers of the three double-headed arrows are at the asterisk. Figure 3c presents all the structural marks of Figure 3b, with their 180° rotational symmetric marks. Namely, I take all the structural

marks from Figure 3b and rotate them by 180° around the asterisk. Figure 3c shows the point-symmetrical structure that I identify in W44, primarily the two bright rims and the two inner filaments.

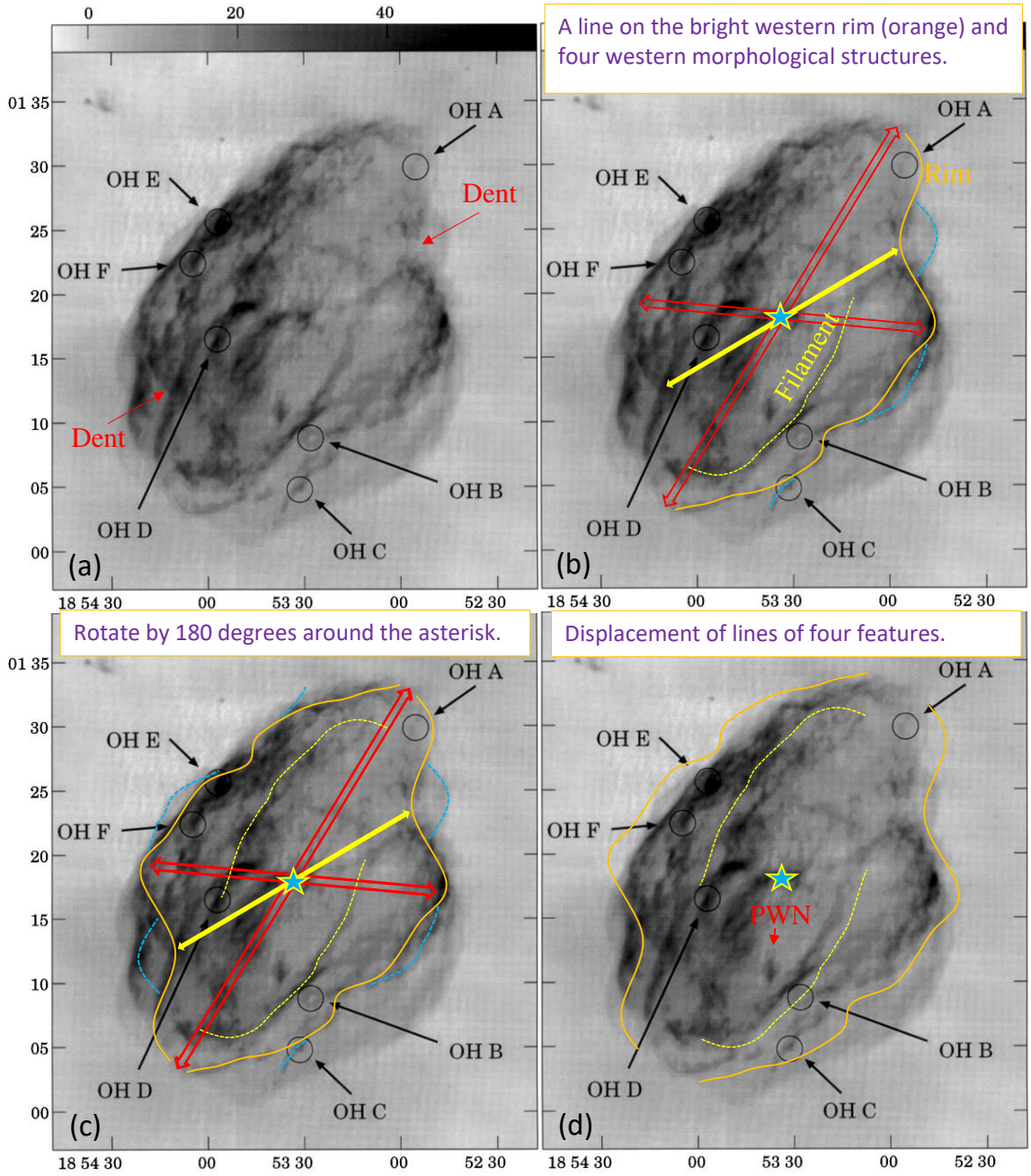

Figure 3. A radio image from [49]. The circles mark strong OH (1720 MHz) emission locations, which I do not refer to in this study. (**a**) The original image from [49]. I added two arrows that point at the two dents. (**b**) My identification of the bright western rim by the orange line. I also mark an inner filament (dotted yellow line) and three structural features outside the western rim (pale blue dashed lines). The two double-line double-headed red arrows are the directions of the two energetic jets that I propose to have shaped W44 during the explosion process. A third pair of jets shaped the inner filaments. (**c**) I copy the structural features I marked on panel (**b**) and rotate by 180° around the point marked by an asterisk. This shows the point-symmetric part of W44. (**d**) I displace outward the marks of the two rims and the two inner filaments to allow visual comparison of the observations with my marks. A short red arrow points at the PWN (pulsar wind nebula). Axes are right ascension and declination (B1950).

To allow a better visual inspection of the rim on the west and east and the two inner filaments, on Figure 3d I displace outward the marks of the two rims and the two inner filaments. I also mark the location of the pulsar-wind nebula (PWN; e.g., [50,51]). This PWN likely influenced the filament on the southwest; hence, I do not expect a perfect point symmetry between the two opposite filaments marked by the dotted yellow lines in Figure 3b–d.

I suggest that each of the two dents are the zones where two jet-inflated structures (bubble/lobes/ears) touch each other on the bright rim. Similar dents are observed between jet-inflated bubbles in some planetary nebulae and clusters of galaxies. In Figure 4, I present an image of the cooling flow cluster RBS 797 from [52]. They mark (white dashed lines) the rims of the four jet-inflated bubbles, i.e., inflated by two pairs of jets. Two adjacent rims have different directions where they meet, forming the dent. The similarity of the structures of the dents in W44 with those in RBS 797, which are known to be inflated by jets, supports the jet-shaped modeling. In the case of the CCSNR W44, more than two pairs of jets were involved. For example, I suggest that a third pair of jets shaped the two opposite filaments.

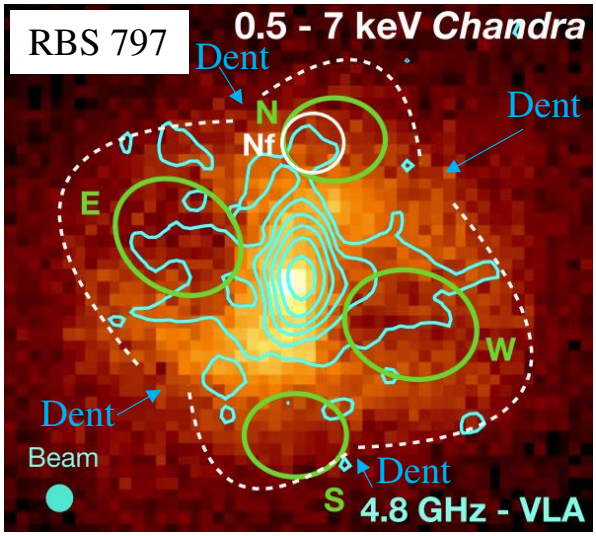

Figure 4. An X-ray image of the cooling flow cluster of galaxy RBS 797 from [52]. Ellipses show the shape of the X-ray cavities. Cyan contours are radio emission at 4.8 GHz from [53]. White dashed arcs encompassing the rims of the bubbles are from their image. Where two rims meet, there is a dent, as I indicate by the four arrows.

4. Answering Possible Counterarguments

Let me answer some possible arguments against my interpretation of a jet-shaped point-symmetrical structure.

(1) Counterargument: There are many filaments and clumps in the radio image of W44, and one can find a point-symmetrical structure just by chance.

Answer: As I indicated above, the point symmetry is not expected to be perfect because of several smearing processes. Considering these smearing processes, I crudely estimate the probability of chance alignment in a point symmetry.

When two opposite jets shape ejecta, they form an axial-symmetric structure. The structure of W44 has a long axis, the long double-headed arrow in Figure 3. To examine the possibility of axial symmetry, in panel b of Figure 5 I mirror the structure I marked on the western side, with the long axis being the mirror. I marked the mirrored structures with dashed lines. It is evident that the bright rim on the east is not a mirror image of the one on the west. Also, only a short segment of the inner filament fits the northeast filament. The dashed blue line matches the bump in the northeast; however, the bump in

the northeast is much brighter and somewhat smaller than that in the northwest. There are some axial-symmetry signatures, but they are not as strong as the point-symmetric ones. The mirror symmetry fails to account for the most prominent morphological features, the dent, nose, and the general rim line. This strengthens the claim for point symmetry.

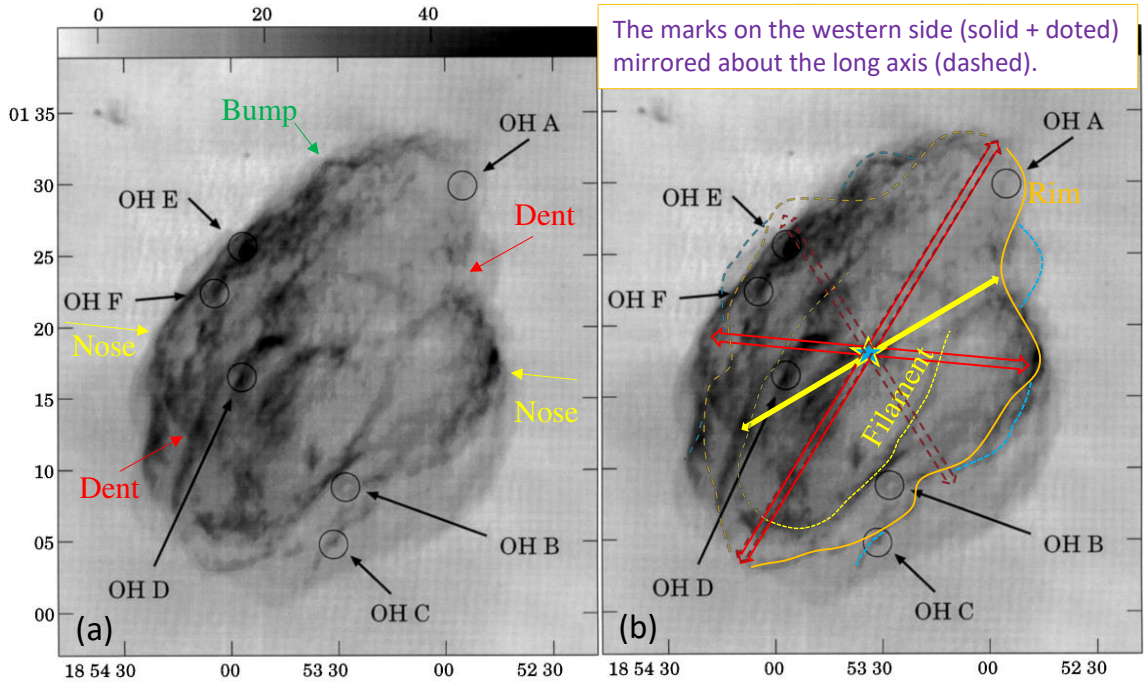

Figure 5. Similar to the first two panels of Figure 3, (**a**) The original image from [49], but on (**b**), the structures marked on the west side are mirrored about the long axis (long double-headed arrow); the mirrored marks are the dashed lines. The bright rims in the west and east are not mirror images.

However, there is still some probability that the point symmetry results from chance alignment. For example, the dent in the southeast is a chance crossing of two filaments. The opening angle of the northwest dent is 130°, while that in the southeast is 120°. The chance of two filaments crossing each other in the southeast within ±10° from the opposite side is $20/180 = 0.11$. However, not only are the angles point-symmetric, but so are the locations of the two dents. Overall, I crudely estimate the chance alignment to a point-symmetric morphology of the bright rims on the two sides, the dents, the noses, and the inner filaments to be <3%, and more likely <1%.

(2) Counterargument: The IR and X-ray images do not show a point-symmetrical structure, as marked on the radio images.

Answer: The IR image (Figure 2) shows many of the structures of the radio image (Figure 3), but not all structures. For example, the IR shows part of the rims but is missing other parts, like the east dent. This situation resembles other point-symmetrical morphologies of CCSNe, e.g., Cassiopeia A's IR and X-ray images reveal point-symmetrical morphologies but do not fully overlap [54]. The X-ray map of W44 shows the inner part, so it does not show the point symmetry of the outer rims. It follows an S-shape morphology [48], a point-symmetrical morphology type, but it seems that the X-ray-emitting gas fills the space inside the rims and filaments.

(3) Counterargument: Interaction with the cloud surrounding W44 shaped its morphology.

Answer: In general, interaction with ambient gas cannot explain the properties of the point-symmetrical structure of CCSNRs [8]. In the case of W44, the protrusions from the dents (pale blue dashed lines) imply that no dense ambient clumps form the dents. Other protrusions outside the rims on both sides show that it is not the ambient medium

that shapes the point-symmetrical morphology. The ambient medium can shape these protrusions; hence, the protrusions are not equal on both sides, i.e., the point symmetry is not perfect. Furthermore, the ambient gas cannot shape the two inner filaments of the point-symmetrical morphology.

(4) Counterargument: Post-explosion jets shaped the point-symmetrical structure. Answer: The point-symmetrical structural features involve the entire CCSNR with an elongated structure. Hence, the energy of the shaping jets must be a large fraction of the explosion energy. It is unlikely that post-explosion jets carry such energy, and it is not clear why post-explosion jets should jitter.

5. Summary

I examined the complicated structure of CCSNR W44 (Figures 1 and 2) by marking some structural features on the west side of a radio image of W44 (Figure 3b), and then rotated it around a central point (the asterisk). The rotated markings overlap with similar structures on the east side (Figure 3c,d), signifying the point-symmetrical morphology of W44. I attribute the shaping of the rims (orange lines) to two pairs of jets (red double-headed arrows). A third pair might have shaped the inner filaments. The dents are the zones where two jet-inflated structures meet. Such jet-shaped dents are observed in planetary nebulae and clusters of galaxies, one of which I present in Figure 4.

In Section 4, I presented answers to some possible counterarguments to my claims. Mainly, I explained why the cloud that CCSNR W44 interacts with cannot account for the point-symmetrical morphology. This interaction instead smears point-symmetrical structures.

The result of this short study, which identifies a point-symmetrical morphology in CCSNR W44, is of great importance to the JJEM. According to the JJEM, stochastic pairs of jets explode most (possibly all) CCSNe, implying an explosion with a point-symmetric morphology. However, most pairs of jets are choked in the core, leaving no observable imprints on the CCSNR morphology. Instabilities during the explosion process, the NS natal kick and a PWN when existing, and interaction with the circumstellar material and the interstellar medium smear point-symmetrical structures that the shaping pairs of jets form. These smearing processes lead to imperfect point-symmetrical morphologies and can even completely erase the point-symmetric structures.

For that, any CCSNR that reveals a point-symmetrical structure is a treasure to the development of the JJEM. SNR W44 is one of only 12 CCSNRs with an identified point-symmetrical morphology [7]. This study shows how a new analysis might reveal a different morphology, motivating more profound studies of CCSNRs for point-symmetrical morphologies.

This study's new identification of a point-symmetrical CCSNR, W44, adds to the growing evidence that the JJEM is the primary explosion process of CCSNe, even when an energetic magnetar supplies extra post-explosion energy (e.g., [55]).

Funding: This research was funded by Pazy Foundation grant number 2020.

Data Availability Statement: The original contributions presented in this study are included in the article. Further inquiries can be directed to the corresponding author(s).

Conflicts of Interest: The author declares no conflict of interest.

References

1. Papish, O.; Soker, N. A planar jittering-jets pattern in core collapse supernova explosions. *Mon. Not. R. Astron. Soc.* **2014**, *443*, 664–670. [CrossRef]
2. Gilkis, A.; Soker, N. Triggering jet-driven explosions of core-collapse supernovae by accretion from convective regions. *Mon. Not. R. Astron. Soc.* **2014**, *439*, 4011–4017. [CrossRef]
3. Shishkin, D.; Soker, N. Supplying angular momentum to the jittering jets explosion mechanism using inner convection layers. *Mon. Not. R. Astron. Soc.* **2021**, *508*, L43–L47. [CrossRef]
4. Shishkin, D. Supplying angular momentum to the jittering jets explosion mechanism using convection in inner star layers. In *Proceedings of the IAU Symposium, IAU Symposium*; Mackey, J., Vink, J.S., St-Louis, N., Eds.; Cambridge University Press: Cambridge, UK, 2024; Volume 361, pp. 607–609. [CrossRef]
5. Wang, N.Y.N.; Shishkin, D.; Soker, N. The Jittering Jets Explosion Mechanism in Electron Capture Supernovae. *Astrophys. J.* **2024**, *969*, 163. [CrossRef]
6. Soker, N. Learning from core-collapse supernova remnants on the explosion mechanism. *arXiv* **2024**, arXiv:2409.13657. [CrossRef]
7. Soker, N. The two alternative explosion mechanisms of core-collapse supernovae: 2024 status report. *arXiv* **2024**, arXiv:2411.08555. [CrossRef]
8. Soker, N.; Shishkin, D. The vela supernova remnant: The unique morphological features of jittering jets. *arXiv* **2024**, arXiv:2409.02626. [CrossRef]
9. Bisnovatyi-Kogan, G.S. The Explosion of a Rotating Star As a Supernova Mechanism. *Soviet Ast.* **1971**, *14*, 652.
10. Bisnovatyi-Kogan, G.S.; Tutukov, A.V. Magnetorotational Supernova Explosions and the Formation of Neutron Stars in Close Binary Systems. *Astron. Rep.* **2004**, *48*, 724–732. [CrossRef]
11. Burrows, A.; Dessart, L.; Livne, E.; Ott, C.D.; Murphy, J. Simulations of Magnetically Driven Supernova and Hypernova Explosions in the Context of Rapid Rotation. *Astrophys. J.* **2007**, *664*, 416–434. [CrossRef]
12. Sawai, H.; Kotake, K.; Yamada, S. Numerical Simulations of Equatorially Asymmetric Magnetized Supernovae: Formation of Magnetars and Their Kicks. *Astrophys. J.* **2008**, *672*, 465–478. [CrossRef]
13. Kuroda, T.; Arcones, A.; Takiwaki, T.; Kotake, K. Magnetorotational Explosion of a Massive Star Supported by Neutrino Heating in General Relativistic Three-dimensional Simulations. *Astrophys. J.* **2020**, *896*, 102. [CrossRef]
14. Aloy, M.Á.; Obergaulinger, M. Magnetorotational core collapse of possible GRB progenitors - II. Formation of protomagnetars and collapsars. *Mon. Not. R. Astron. Soc.* **2021**, *500*, 4365–4397. [CrossRef]
15. Kondratyev, I.A.; Moiseenko, S.G.; Bisnovatyi-Kogan, G.S. Magnetorotational neutron star kicks. *arXiv* **2024**, arXiv:2410.09521. [CrossRef]
16. Shibagaki, S.; Kuroda, T.; Kotake, K.; Takiwaki, T.; Fischer, T. Three-dimensional GRMHD simulations of rapidly rotating stellar core collapse. *Mon. Not. R. Astron. Soc.* **2024**, *531*, 3732–3743. [CrossRef]
17. Zha, S.; Müller, B.; Powell, J. Nucleosynthesis in the Innermost Ejecta of Magnetorotational Supernova Explosions in 3-dimensions. *arXiv* **2024**, arXiv:2403.02072. [CrossRef]
18. Gilkis, A. Asymmetric Core-collapse of a Rapidly-rotating Massive Star. In Proceedings of the The Lives and Death-Throes of Massive Stars, IAU Symposium, Auckland, NZ, USA, 28 November–2 December 2017; Eldridge, J.J., Bray, J.C., McClelland, L.A.S., Xiao, L., Eds.; Cambridge University Press: Cambridge, UK, 2017; Volume 329, p. 400. [CrossRef]
19. Müller, B. Supernova Simulations. *arXiv* **2024**, arXiv:2403.18952. [CrossRef]
20. Smirnova, T.V.; Shishov, V.I.; Malofeev, V.M. The Spatial Structure of Pulsar Emission Sources Determined Using Interstellar Scintillation. *Astrophys. J.* **1996**, *462*, 289. [CrossRef]
21. Johnston, S.; Hobbs, G.; Vigeland, S.; Kramer, M.; Weisberg, J.M.; Lyne, A.G. Evidence for alignment of the rotation and velocity vectors in pulsars. *Mon. Not. R. Astron. Soc.* **2005**, *364*, 1397–1412. [CrossRef]
22. Noutsos, A.; Kramer, M.; Carr, P.; Johnston, S. Pulsar spin-velocity alignment: Further results and discussion. *Mon. Not. R. Astron. Soc.* **2012**, *423*, 2736–2752. [CrossRef]
23. Bear, E.; Shishkin, D.; Soker, N. The Puppis A supernova remnant: An early jet-driven neutron star kick followed by jittering jets. *arXiv* **2024**, arXiv:2409.11453. [CrossRef]
24. Winteler, C.; Käppeli, R.; Perego, A.; Arcones, A.; Vasset, N.; Nishimura, N.; Liebendörfer, M.; Thielemann, F.K. Magnetorotationally Driven Supernovae as the Origin of Early Galaxy r-process Elements? *Astrophys. J.* **2012**, *750*, L22. [CrossRef]
25. Abdo, A.A.; Ackermann, M.; Ajello, M.; Baldini, L.; Ballet, J.; Barbiellini, G.; Baring, M.G.; Bastieri, D.; Baughman, B.M.; Bechtol, K.; et al. Gamma-Ray Emission from the Shell of Supernova Remnant W44 Revealed by the Fermi LAT. *Science* **2010**, *327*, 1103. [CrossRef] [PubMed]
26. Jones, L.R.; Smith, A.; Angelini, L. A detailed X-ray and radio study of the supernova remnant W 44. *Mon. Not. R. Astron. Soc.* **1993**, *265*, 631–640. [CrossRef]
27. Shelton, R.L.; Kuntz, K.D.; Petre, R. Chandra Observations and Models of the Mixed-Morphology Supernova Remnant W44: Global Trends. *Astrophys. J.* **2004**, *611*, 906–918. [CrossRef]

28. Kawasaki, M.; Ozaki, M.; Nagase, F.; Inoue, H.; Petre, R. Ionization States and Plasma Structures of Mixed-Morphology Supernova Remnants Observed with ASCA. *Astrophys. J.* **2005**, *631*, 935–946. [CrossRef]
29. Uchida, H.; Koyama, K.; Yamaguchi, H.; Sawada, M.; Ohnishi, T.; Tsuru, T.G.; Tanaka, T.; Yoshiike, S.; Fukui, Y. Recombining Plasma and Hard X-Ray Filament in the Mixed-Morphology Supernova Remnant W 44. *Publ. Astron. Soc. Jpn.* **2012**, *64*, 141. [CrossRef]
30. Okon, H.; Tanaka, T.; Uchida, H.; Yamaguchi, H.; Tsuru, T.G.; Seta, M.; Smith, R.K.; Yoshiike, S.; Orlando, S.; Bocchino, F.; et al. Deep XMM-Newton Observations Reveal the Origin of Recombining Plasma in the Supernova Remnant W44. *Astrophys. J.* **2020**, *890*, 62. [CrossRef]
31. Rho, J.; Petre, R.; Schlegel, E.M.; Hester, J.J. An X-Ray and Optical Study of the Supernova Remnant W44. *Astrophys. J.* **1994**, *430*, 757. [CrossRef]
32. Giacani, E.B.; Dubner, G.M.; Kassim, N.E.; Frail, D.A.; Goss, W.M.; Winkler, P.F.; Williams, B.F. New Radio and Optical Study of the Supernova Remnant W44. *Astron. J.* **1997**, *113*, 1379. [CrossRef]
33. Mavromatakis, F.; Boumis, P.; Goudis, C.D. The faint supernova remnant G 34.7-0.4 (W44). *Astron. Astrophys.* **2003**, *405*, 591–596. [CrossRef]
34. Reach, W.T.; Rho, J.; Jarrett, T.H. Shocked Molecular Gas in the Supernova Remnants W28 and W44: Near-Infrared and Millimeter-Wave Observations. *Astrophys. J.* **2005**, *618*, 297–320. [CrossRef]
35. Reach, W.T.; Rho, J.; Tappe, A.; Pannuti, T.G.; Brogan, C.L.; Churchwell, E.B.; Meade, M.R.; Babler, B.; Indebetouw, R.; Whitney, B.A. A Spitzer Space Telescope Infrared Survey of Supernova Remnants in the Inner Galaxy. *Astron. J.* **2006**, *131*, 1479–1500. [CrossRef]
36. Seta, M.; Hasegawa, T.; Sakamoto, S.; Oka, T.; Sawada, T.; Inutsuka, S.i.; Koyama, H.; Hayashi, M. Detection of Shocked Molecular Gas by Full-Extent Mapping of the Supernova Remnant W44. *Astron. J.* **2004**, *127*, 1098–1116. [CrossRef]
37. Hoffman, I.M.; Goss, W.M.; Brogan, C.L.; Claussen, M.J. The OH (1720 MHz) Supernova Remnant Masers in W44: MERLIN and VLBA Polarization Observations. *Astrophys. J.* **2005**, *627*, 803–812. [CrossRef]
38. Castelletti, G.; Dubner, G.; Brogan, C.; Kassim, N.E. The low-frequency radio emission and spectrum of the extended SNR W44: New VLA observations at 74 and 324 MHz. *Astron. Astrophys.* **2007**, *471*, 537–549. [CrossRef]
39. Anderl, S.; Gusdorf, A.; Güsten, R. APEX observations of supernova remnants. I. Non-stationary magnetohydrodynamic shocks in W44. *Astron. Astrophys.* **2014**, *569*, A81. [CrossRef]
40. Egron, E.; Pellizzoni, A.; Iacolina, M.N.; Loru, S.; Marongiu, M.; Righini, S.; Cardillo, M.; Giuliani, A.; Mulas, S.; Murtas, G.; et al. Imaging of SNR IC443 and W44 with the Sardinia Radio Telescope at 1.5 and 7 GHz. *Mon. Not. R. Astron. Soc.* **2017**, *470*, 1329–1341. [CrossRef]
41. Loru, S.; Pellizzoni, A.; Egron, E.; Righini, S.; Iacolina, M.N.; Mulas, S.; Cardillo, M.; Marongiu, M.; Ricci, R.; Bachetti, M.; et al. Investigating the high-frequency spectral features of SNRs Tycho, W44, and IC443 with the Sardinia Radio Telescope. *Mon. Not. R. Astron. Soc.* **2019**, *482*, 3857–3867. [CrossRef]
42. Seta, M.; Hasegawa, T.; Dame, T.M.; Sakamoto, S.; Oka, T.; Handa, T.; Hayashi, M.; Morino, J.I.; Sorai, K.; Usuda, K.S. Enhanced CO J = 2-1/J = 1-0 Ratio as a Marker of Supernova Remnant-Molecular Cloud Interactions: The Cases of W44 and IC 443. *Astrophys. J.* **1998**, *505*, 286–298. [CrossRef]
43. Nobukawa, K.K.; Nobukawa, M.; Koyama, K.; Yamauchi, S.; Uchiyama, H.; Okon, H.; Tanaka, T.; Uchida, H.; Tsuru, T.G. Evidence for a Neutral Iron Line Generated by MeV Protons from Supernova Remnants Interacting with Molecular Clouds. *Astrophys. J.* **2018**, *854*, 87. [CrossRef]
44. Koo, B.C.; Kim, C.G.; Park, S.; Ostriker, E.C. Radiative Supernova Remnants and Supernova Feedback. *Astrophys. J.* **2020**, *905*, 35. [CrossRef]
45. Liu, M.; Hu, Y.; Lazarian, A. Velocity gradients: Magnetic field tomography towards the supernova remnant W44. *Mon. Not. R. Astron. Soc.* **2022**, *510*, 4952–4961. [CrossRef]
46. Cosentino, G.; Tan, J.C.; Jiménez-Serra, I.; Fontani, F.; Caselli, P.; Henshaw, J.D.; Barnes, A.T.; Law, C.Y.; Viti, S.; Fedriani, R.; et al. Deuterium fractionation across the infrared-dark cloud G034.77–00.55 interacting with the supernova remnant W44. *Astron. Astrophys.* **2023**, *675*, A190. [CrossRef]
47. Wolszczan, A.; Cordes, J.M.; Dewey, R.J. Discovery of a Young, 267 Millisecond Pulsar in the Supernova Remnant W44. *Astrophys. J.* **1991**, *372*, L99. [CrossRef]
48. Grichener, A.; Soker, N. Core collapse supernova remnants with ears. *Mon. Not. R. Astron. Soc.* **2017**, *468*, 1226–1235. [CrossRef]
49. Claussen, M.J.; Frail, D.A.; Goss, W.M.; Gaume, R.A. Polarization Observations of 1720 MHz OH Masers toward the Three Supernova Remnants W28, W44, and IC 443. *Astrophys. J.* **1997**, *489*, 143–159. [CrossRef]
50. Frail, D.A.; Giacani, E.B.; Goss, W.M.; Dubner, G. The Pulsar Wind Nebula around PSR B1853+01 in the Supernova Remnant W44. *Astrophys. J.* **1996**, *464*, L165. [CrossRef]
51. Petre, R.; Kuntz, K.D.; Shelton, R.L. The X-Ray Structure and Spectrum of the Pulsar Wind Nebula Surrounding PSR B1853+01 in W44. *Astrophys. J.* **2002**, *579*, 404–410. [CrossRef]

52. Ubertosi, F.; Gitti, M.; Brighenti, F.; Brunetti, G.; McDonald, M.; Nulsen, P.; McNamara, B.; Randall, S.; Forman, W.; Donahue, M.; et al. The Deepest Chandra View of RBS 797: Evidence for Two Pairs of Equidistant X-ray Cavities. *Astrophys. J.* **2021**, *923*, L25. [CrossRef]
53. Gitti, M.; Giroletti, M.; Giovannini, G.; Feretti, L.; Liuzzo, E. A candidate supermassive binary black hole system in the brightest cluster galaxy of RBS 797. *Astron. Astrophys.* **2013**, *557*, L14. [CrossRef]
54. Bear, E.; Soker, N. Identifying a point-symmetric morphology in supernova remnant Cassiopeia A: Explosion by jittering jets. *New Astron.* **2025**, *114*, 102307. [CrossRef]
55. Kumar, A. Insights from Modeling Magnetar-driven Light Curves of Stripped-envelope Supernovae. *arXiv* **2024**, arXiv:2412.09357. [CrossRef]